Solid Earth

Open Access

EGU

Supplement of

Correcting for static shift of magnetotelluric data with airborne electromagnetic measurements: a case study from Rathlin Basin, Northern Ireland

Robert Delhaye et al.

Correspondence to: Robert Delhaye (rdelhaye@cp.dias.ie)

S1 Comparison with Inversion of Non-rotated Data and Mesh

In order to establish if the choice of mesh and data rotation significantly influences the resulting models, a further comparative inversion was performed using non-rotated data and mesh. The non-rotated mesh comprised $64 \times 80 \times 82$ cells in size (X,Y,Z), with cells in the central portion of the model of lateral extent 400 m by 400 m. The layer thicknesses, initial halfspace resistivity of 30 Ωm, bathymetry and smoothing factors were kept identical to the rotated mesh used within the article. Similarly, the same selection of data and error floors as used for the rotated data were applied to the non-rotated data. The resulting models, N_c (i.e., inverted from static shift-corrected, non-rotated data) and N_o (i.e., inverted from original, non-rotated data), had normalised RMS misfits of 2.14 (63 iterations) and 2.17 (60 iterations) respectively.

Figures S1, S3, S5 and S7 present the diagnostic images of resistivity, Δ (the logarithmic resistivity difference), and the normalised cross-gradient value for the two models M_c and M_o determined for rotated data and meshes. In contrast, S2, S4, S6 and S8 present the same diagnostic images for the comparative models N_c and N_o determined for non-rotated data and meshes. By examining the resistivity plots of N_c in comparison to the resistivity plots of M_c, it is clear that the non-rotated N models recover generally similar structures to their rotated M counterparts, with an extensive central conductor in N_c of similar extent to the central conductor in M_c associated with the Permian and Triassic sediments. Similarly, both M and N models feature a large resistor in the south-east associated with the Dalradian metasedimentary block. Although it is apparent that the non-rotated models have resolved slightly less structure at depth than the rotated models, the discussion presented here is not intended to be a comprehensive overview of the topic of model and data rotation. For detailed investigation of the effects of rotation on MT inversion, the reader is referred to other works such as Tietze and Ritter (2013).

As the mesh and data rotation does affect 3D inversion results, it is the changes in Δ, the logarithmic difference between N_c and N_o, that are of most interest to this research. The small variations between the resistivity images of N_c and M_c have the consequence that the distributions of Δ are not expected to be identical, as can be clearly seen. The rotated models M show elevated values of Δ, extending to greater depths than in the non-rotated models N. With the caveat that the resistivity distributions cannot be declared equivalent between the M and N models (i.e., the differences observed between N and M models cannot be categorically defined as purely due to rotation), it appears that rotation of the inversion mesh and data exaggerate the effects of static shift correction on the resulting model. For example, if the depth slices from 1550 m are considered, the distributions of Δ for the rotated models M generally show magnitudes that are elevated approximately a quarter of an order of magnitude greater than those of the non-rotated models N. It should be noted that even with the reduced magnitudes of Δ in the non-rotated N models, the effects of

static shift correction still propagate to 2 km depth within the models.

References

Tietze, K. and Ritter, O.: Three-dimensional magnetotelluric inversion in practice the electrical conductivity structure of the San Andreas Fault in Central California, Geophysical Journal International, 195, 130, doi: 10.1093/gji/ggt234, 2013.
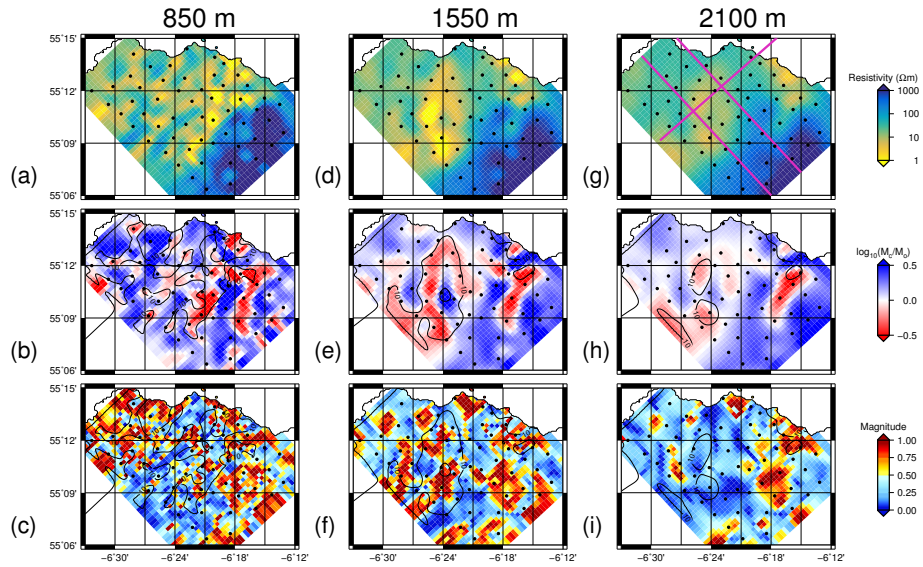
Figure S1: Top row shows resistivity slices through the rotated, static shift corrected model M_c taken at 850 (a), 1550 (d) and 2100 (g) metres below sea level. Middle row shows the resistivity difference Δ between the non-rotated models in decades $(\Delta(M_c, M_o) = \log_{10}(M_c/M_o))$ for the same depths, where red shows M_c more conductive than M_o, and blue more resistive. Bottom row shows the magnitude of the normalised cross-gradient (the cross product of the gradient vectors of models ∇M_c and ∇M_o) as a diagnostic of structural similarity between the models, with 0 (blue) showing parallel gradient vectors (i.e., very similar structure), and 1 (red) showing orthogonal gradient vectors and structural disagreement. The difference and cross-gradient plots are overlain by the 10 Ωm contour from the corresponding resistivity slice. Magenta lines on subplot (g) indicate the location of Profiles A, B and C.
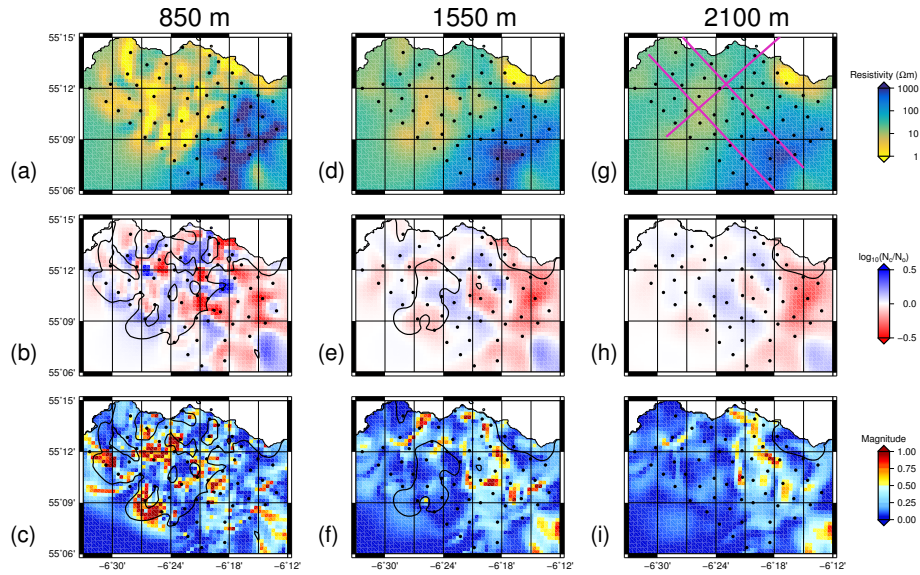
Figure S2: Top row shows resistivity slices through the non-rotated, static shift corrected model N_c taken at 850 (a), 1550 (d) and 2100 (g) metres below sea level. Middle row shows the resistivity difference Δ between the non-rotated models in decades $(\Delta(N_c, N_o) = \log_{10}(N_c/N_o))$ for the same depths, where red shows N_c more conductive than N_o, and blue more resistive. Bottom row shows the magnitude of the normalised cross-gradient (the cross product of the gradient vectors of models ∇N_c and ∇N_o) as a diagnostic of structural similarity between the models, with 0 (blue) showing parallel gradient vectors (i.e., very similar structure), and 1 (red) showing orthogonal gradient vectors and structural disagreement. The difference and cross-gradient plots are overlain by the 10 Ωm contour from the corresponding resistivity slice. Magenta lines on subplot (g) indicate the location of Profiles A, B and C.

4
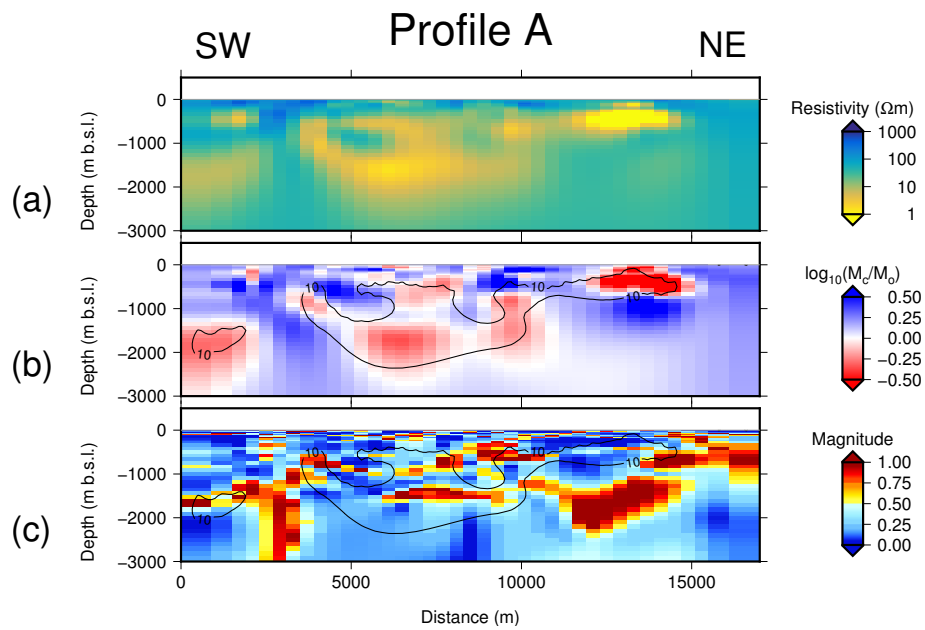
Figure S3: Profile A taken along the axis of the concealed basin through the static shift corrected resistivity model M_c (location shown on Figures S1g and S2g). The resistivity is shown in (a), the resistivity difference $\Delta(M_c, M_o)$ is shown in (b), and the cross-gradient of M_c and M_o is shown in (c). Contours on the difference and cross-gradient plots show the 10 Ωm contour. For presentation a vertical exaggeration of 1.5 is used.
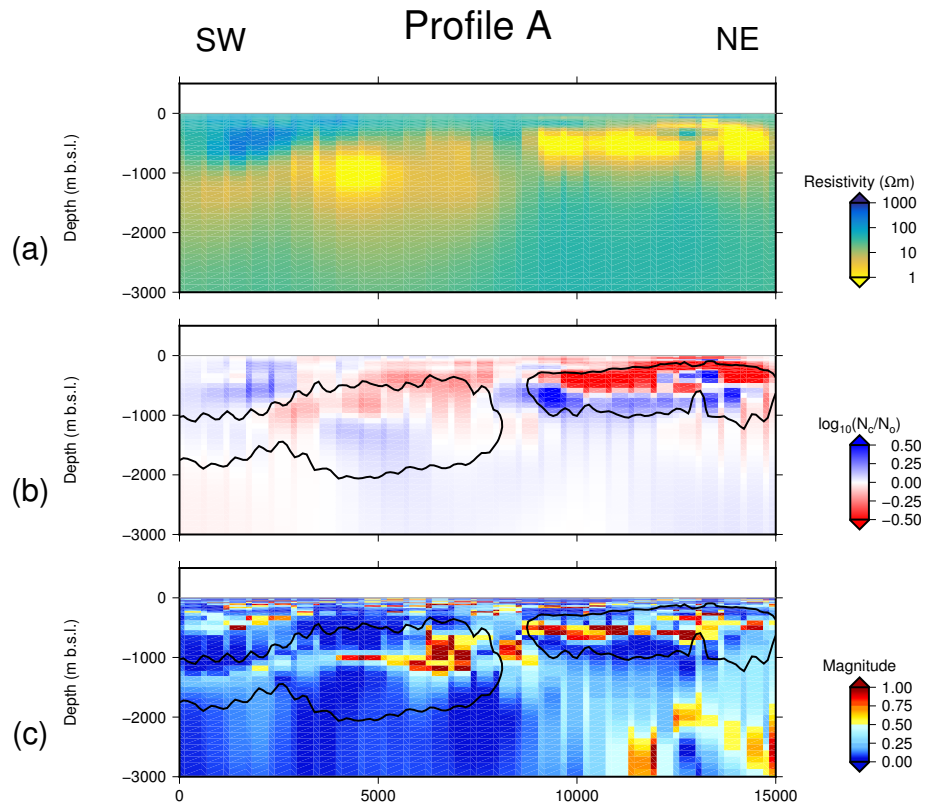
Figure S4: Profile A taken along the axis of the concealed basin through the non-rotated, static shift corrected resistivity model N_c (location shown on Figures S1g and S2g). The resistivity is shown in (a), the resistivity difference $\Delta(N_c, N_o)$ is shown in (b), and the cross-gradient of N_c and N_o is shown in (c). Contours on the difference and cross-gradient plots show the 10 Ωm contour. For presentation a vertical exaggeration of 1.5 is used.
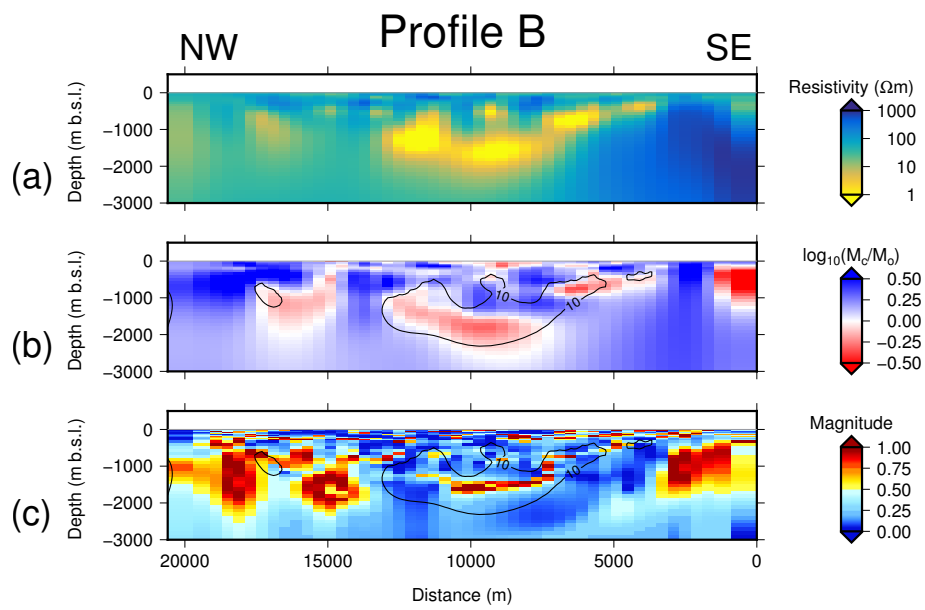
Figure S5: Profile B taken across the static shift corrected resistivity model M_c (location shown on Figures S1g and S2g). The resistivity is shown in (a), the resistivity difference $\Delta(M_c, M_o)$ is shown in (b), and the cross-gradient of M_c and M_o is shown in (c). Contours on the difference and cross-gradient plots show the 10 Ωm contour. For presentation a vertical exaggeration of 1.5 is used.
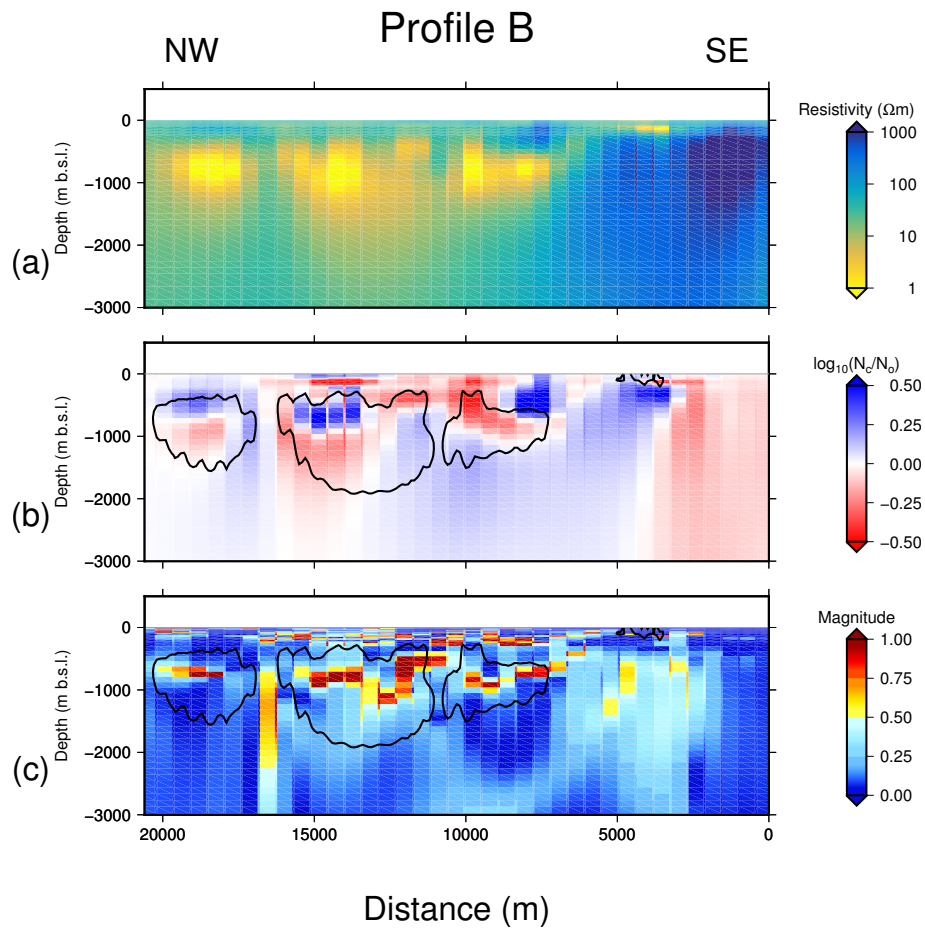
Figure S6: Profile B taken across the non-rotated, static shift corrected resistivity model N_c (location shown on Figures S1g and S2g). The resistivity is shown in (a), the resistivity difference $\Delta(M_c, M_o)$ is shown in (b), and the cross-gradient of N_c and N_o is shown in (c). Contours on the difference and cross-gradient plots show the 10 Ωm contour. For presentation a vertical exaggeration of 1.5 is used.
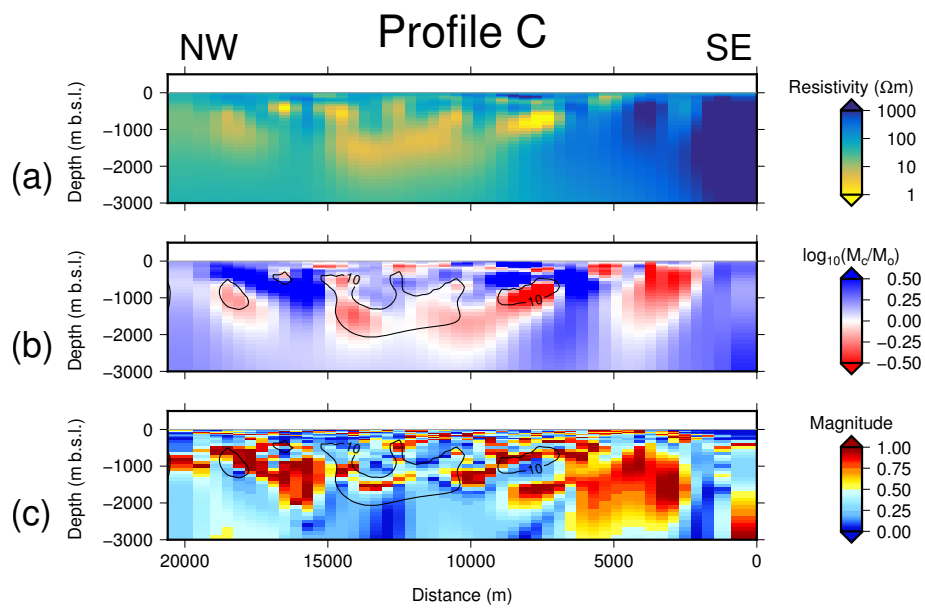
Figure S7: Profile C taken across the static shift corrected resistivity model M_c (location shown on Figures S1g and S2g). The resistivity is shown in (a), the resistivity difference $\Delta(M_c, M_o)$ is shown in (b), and the cross-gradient of M_c and M_o is shown in (c). Contours on the difference and cross-gradient plots show the 10 Ωm contour. For presentation a vertical exaggeration of 1.5 is used.

9
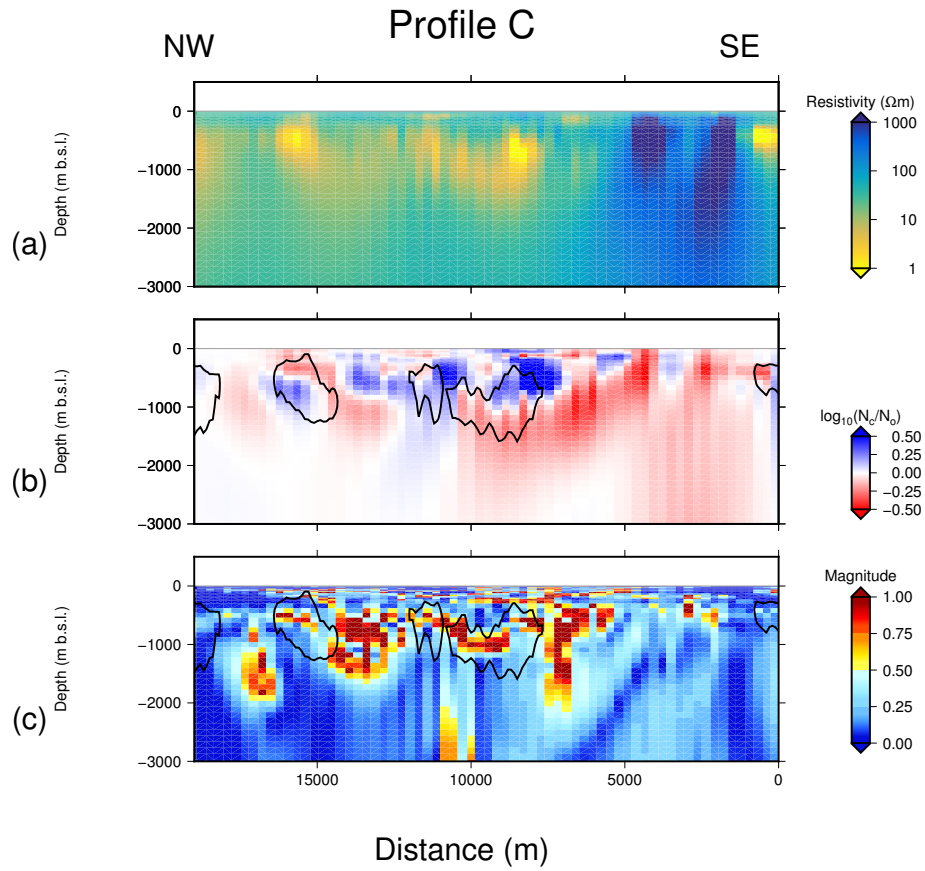
Figure S8: Profile C taken across the non-rotated, static shift corrected resistivity model N_c (location shown on Figures S1g and S2g). The resistivity is shown in (a), the resistivity difference $\Delta(N_c, N_o)$ is shown in (b), and the cross-gradient of N_c and N_o is shown in (c). Contours on the difference and cross-gradient plots show the 10 Ωm contour. For presentation a vertical exaggeration of 1.5 is used.

10